

A  $\text{Mn}^{\text{II}}_{12}$  Supramolecular Array with Four Independent Spin-Coupled SubunitsKonstantin V. Shuvaev,<sup>[a]</sup> Louise N. Dawe,<sup>[a]</sup> and Laurence K. Thompson\*<sup>[a]</sup>**Keywords:** Ligand design / Polytopic ligands / Self-assembly / Grid structure / Supramolecular chemistry / Manganese / Copper

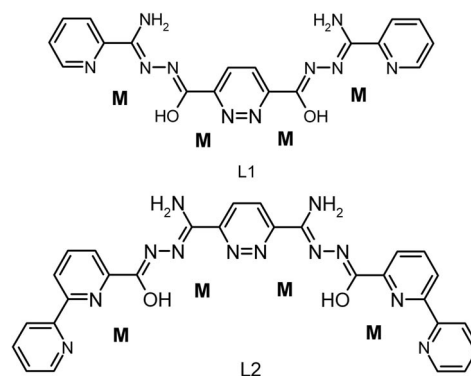
The tetratopic pyridazine-hydrazone ligand L2 is based on a design that successfully produces self-assembled  $[4 \times 4] \text{M}^{\text{II}}_{16}$  ( $\text{M} = \text{Mn}, \text{Cu}$ ) grids, but incorporates  $\pi$ -charge-rich, strong field bipy end groups. L2 forms an unusual incomplete

“super” triangular  $\text{Cu}^{\text{II}}_{11}$  motif, dominated by the bipy ends. We now describe the incomplete  $\text{Mn}^{\text{II}}_{12}$  partial grid  $[\text{Mn}_{12}(\text{L2-2H})_6(\text{L-H})_2\{\text{N}(\text{CN})_2\}_2]$ .

## Introduction

The design of polytopic ligands capable of directed synthesis of specific polynuclear architectures is highly desirable in the quest for novel metal clusters with potentially useful properties, e.g. electronic, magnetic, photo-chemical etc. Electron-rich  $[\text{n} \times \text{n}]$  square transition metal grids are attractive platforms, and many examples with nuclearities in the range  $n = 2\text{--}5$  have been produced.<sup>[1–9]</sup> The flat nature of the grids lends them to surface applications, with the potential for device application.<sup>[2,6,9]</sup> Pyridazine hydrazone-based ligands, e.g. L1, have four contiguous pockets with the potential for formation of five-membered chelate rings on coordination (Scheme 1), and have produced numerous heteroleptic  $\text{Mn}^{\text{II}}_{16}$  and  $\text{Cu}^{\text{II}}_{16}$   $[4 \times 4]$  examples,<sup>[1,7,8,10]</sup> exhibiting intramolecular antiferromagnetic and ferromagnetic exchange, respectively. The grids comprise  $[\text{M}_4(\mu\text{-O})_4]$  squares, created from the two end pockets, with each square linked to a neighbour by a combination of  $\mu$ -pyridazine/ $\mu$ -O, where the extra bridge is scavenged from the solvent (e.g.  $\text{OH}^-$ ,  $\text{O}^{2-}$ ,  $\text{H}_2\text{O}$ ). The bent nature of the ligand pockets does not deter grid formation. A common feature of all the grids is the close proximity of the metal ions, brought to bear by short range bridging contacts ( $\mu\text{-O}$ ), and also the concomitant close separation of the ligand aromatic rings (3.5–4.0 Å). Grid twists are observed in response to the offset nature of the  $\pi\text{--}\pi$  contacts (slipped face contacts). Such interactions occur in addition to the metal–ligand covalent bonding contacts resulting from the pre-organized self-assembly of the grids, and so cannot be considered in isolation. However, such interactions are clearly of importance in the overall thermodynamic balance for the assembly process.  $\pi\text{--}\pi$  interactions contribute to the organization of self-

assembled structures and superstructures in general, and occur in biological systems (e.g. DNA base pair interactions), and have been identified in host–guest complexes involving  $\text{C}_{60}$  and related systems. Interaction energies approach  $50 \text{ kJ mol}^{-1}$ .<sup>[11]</sup> A recent report highlights the effect of  $\text{Zn}^{\text{II}}$  concentration on the balance of  $\pi$ -stacking associations and coordination effects involving a bis(imidazolyl-carbazole) ligand (L). At low  $\text{Zn}^{\text{II}}$  concentration the formation of the  $[\text{L}_4\text{Zn}^{2+}]_2$  dimer occurs through dominant  $\pi$ -interactions via the carbazole moiety, which are eliminated at higher  $\text{Zn}^{\text{II}}$  concentrations as  $[(\text{L}_3)\text{Zn}^{2+}]$  forms.<sup>[12]</sup>



Scheme 1. Tetratopic bis(hydrazone) ligands.

The isomeric tetratopic pyridine hydrazone ligand L2 differs from L1, with four contiguous tridentate pockets, but is modified with strong field terminal bipy groups. The ligand groupings would bend in the opposite sense if a similar grid assembly formed. L2 produces a most unusual  $\text{Cu}^{\text{II}}_{11}$  cluster **1** with a double triangular motif (Figure S1), in which the bipy ends dominate the assembly by aggregating at the corners forming  $\text{Cu}_2$  subunits with close  $\pi\text{--}\pi$  bipy contacts. The pyridazine segments form the sides of the triangle, with pairs of  $\text{Cu}^{\text{II}}$  ions bound by the pyridazines on two sides, but with only one on the third side, resulting from a pronounced twist in the ligand backbone.<sup>[13]</sup>

[a] Department of Chemistry, Memorial University, St. John's, Newfoundland, A1B 3X7, Canada  
Fax: +1-709-737-3702  
E-mail: lk.thompson@mun.ca

Supporting information for this article is available on the WWW under <http://dx.doi.org/10.1002/ejic.201000837>.

## Results and Discussion

Reaction of  $\text{Mn}(\text{NO}_3)_2$  with L2 in the presence of  $\text{N}(\text{CN})_2^-$  produced orange crystals of  $[\text{Mn}_{12}(\text{L}2\text{-}2\text{H})_6(\text{L-H})_2\{\text{N}(\text{CN})_2\}_2](\text{NO}_3)_8(\text{H}_2\text{O})_{24}$  (**2**) (Figure 1).

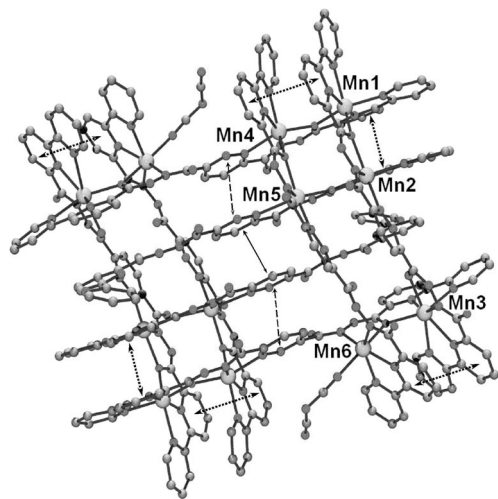


Figure 1. Molecular structure of **2**, with  $\pi$  contacts highlighted (small hatched arrows – bipy; solid and large hatched arrows – pyridazine).

The self-assembled product is a dodecanuclear cation consisting of four essentially independent subunits; two identical  $[\text{Mn}_4(\mu\text{-O})_4]$   $[2 \times 2]$  squares, and two identical  $[\text{Mn}_2(\mu\text{-O})_2]$  dinuclear fragments, related by inversion symmetry, arranged in two well separated halves of the structure (Figure 2 shows the square and dinuclear subunits).

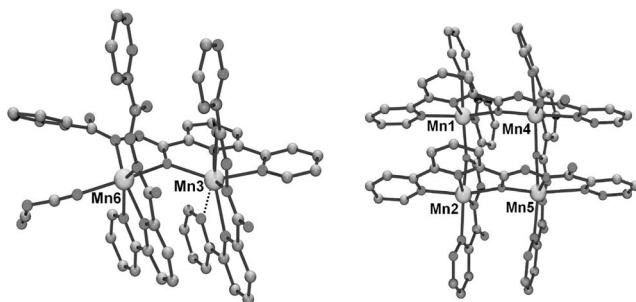


Figure 2. Dinuclear (a) and tetranuclear (b) fragments in **2**.

The ligands are arranged in two groupings, with roughly parallel pairs forming the backbone of each main fragment. Four other ligands span the two halves, with the outer two linking tetranuclear and dinuclear fragments. The central pyridazines do not bridge, as is typical in other systems, and just coordinate in a monodentate fashion, resulting from a  $180^\circ$  ligand twist. What is remarkable, and what appears to play a significant role in the assembly process, is the internal columnar-like stack of pyridazine rings (Figure 1), with very close ring–ring contacts. The rings occur in two pairs (large hatched arrows) offset by  $11.8^\circ$ , each separated by  $3.573(2)$  Å. The pairs are mutually oriented by  $180^\circ$ , with a  $3.654(2)$  Å separation between the pairs and an offset of  $27.9^\circ$  (solid arrow) (ring centroid references). Also remark-

able is the apparent freezing of two largely uncoordinated ligands (middle two of the group) within the structure, bound only at one end in a bidentate  $\mu\text{-O}$ -bridging fashion to Mn2 and Mn5 (and symmetry related metal ions). The uncoordinated bipy ends project well beyond the edge of the molecule, held in place in part by additional  $\pi$  contacts with adjacent bipy rings [Figure S3;  $3.562(3)$  Å,  $3.609(3)$  Å separations]. Within each  $[2 \times 2]$  square Mn1, Mn2 and Mn4 are six-coordinate, with Mn–L distances in the range  $2.12\text{--}2.36$  Å. Mn3 has one long contact to a pyridazine ring nitrogen atom ( $2.54$  Å), and could be considered to be square-pyramidal. Within each dinuclear subunit Mn6 is six-coordinate (Mn–L  $2.12\text{--}2.35$  Å), while Mn3 is highly distorted with one long possible additional contact ( $2.70$  Å) to the terminal pyridine, and six shorter Mn–L contacts ( $2.21\text{--}2.42$  Å). Slipped face bipy contacts [Figure 1, small hatched arrows;  $3.533(2)$  Å,  $3.699(2)$  Å; offset angles  $20.0^\circ$ ,  $27.3^\circ$ ] also exist within the tetranuclear and dinuclear fragments.

The two dicyanamide ions bind in a simple monodentate fashion, and are unlikely to have exerted a significant role in the assembly process, and just fill vacant coordination sites. What is more likely the reason for such an unusual assembly is the steric crowding which would occur if four  $[2 \times 2]$  square corners existed on the same side of the ligands, bridged by the pyridazines (Scheme 1), as would be typical of the  $\text{M}_{16}$  square grids formed by ligands like L1. The grid-based information encoded in the ligand directs the assembly based on coordination driving forces of the  $\mu\text{-O}$ -bridging interactions, and the arrangement of ligands in roughly parallel groupings driven by  $\pi$  interactions. The ligand twists by  $180^\circ$  around the pyridazine groups are clearly a result of the clashes which would occur between the four  $\text{M}_4$  square subunits in a putative  $[4 \times 4]$  grid assembly. The collective assembly-driven forces thus include multiple  $\pi$  contacts (see Figures S2, S3; Tables S1, S2) and the  $\mu\text{-O}$ -bridging interactions, which are opposing the various steric constraints associated with the bent nature of the ligand pocket arrangement. Clearly, a balance of these effects leads to the final structural motif.

The extended association of complex polymetallic assemblies is seen as a potentially useful attribute when global cooperative interactions are considered (e.g. coherence, decoherence effects, spin entanglement etc. in systems with potential for quantum information processing). In this context  $\pi$  contacts and H-bonding contacts may play an important role, if for no other reason than to add an additional element of organization, which could be exploited in e.g. the formation of a close packed monolayer assembly on a surface. Examination of intermolecular contacts in **2** reveals both  $\text{CO}\cdots\text{H}_2\text{N}$  contacts [Figure S4;  $2.967(5)$  Å] and also slipped-face  $\pi$  contacts between individual clusters (Figure S5).

Within each  $\text{Mn}^{\text{II}}_4$  square and each  $\text{Mn}^{\text{II}}_2$  grouping (Figure 2) the metal centres are bridged just by  $\mu\text{-O}$  atoms from enolic hydrazone fragments. Mn–O–Mn bridge angles fall into a narrow range ( $128.3\text{--}132.6^\circ$ ), suggesting comparable magnetic spin exchange via each bridge. Variable tempera-

ture magnetic data (Figure 3) show a smooth drop in moment (per mol) from 19.8  $\mu_B$  at 300 K to 3.7  $\mu_B$  at 2 K, consistent with twelve Mn<sup>II</sup> centres exhibiting intramolecular antiferromagnetic exchange ( $\mu_{SO} = 20.5 \mu_B$ ). The symmetry of the Mn<sub>12</sub> assembly, coupled with the similarity in Mn–O–Mn bridge angles, suggests that the exchange model can be simplified to the sum of two square and two dinuclear sub-units with the same  $J$  value [Equation (1)], scaled to Mn<sub>12</sub>.

$$H_{\text{ex}} = -J\{S_1S_2 + S_2S_3 + S_3S_4 + S_1S_4\} - J\{S_5S_6\} \quad (1)$$

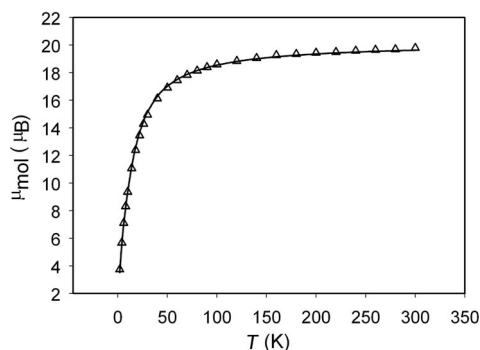


Figure 3. Variable temperature magnetic data for **2**. The solid line was calculated from eqn. (1) with  $g_{\text{av}} = 1.98$ ,  $J = -2.4 \text{ cm}^{-1}$ .

A good fit of the data to Equation (1) using MAGMUN4.11<sup>[14]</sup> gave  $g_{\text{av}} = 1.98$ ,  $J = -2.4 \text{ cm}^{-1}$ ,  $10^2 R = 3.8 \{R = [\Sigma(\chi_{\text{obs}} - \chi_{\text{calc}})^2 / \Sigma\chi_{\text{obs}}^2]^{1/2}\}$ . The  $J$  value is consistent with similar  $[2 \times 2]$  tetranuclear subunits, based on related ditopic ligands.<sup>[5]</sup> The good fit to the simple exchange model indicates clearly that the four spin exchanged subunits are magnetically remote, as would be predicted from the structure.

## Conclusions

Ligand design, with the ultimate formation of predictable polymetallic architectures by a convergent assembly process has enjoyed considerable success with relatively simple polytopic hydrazone ligands, with  $[n \times n]$  square grid examples spanning the range  $n = 2$ –5.<sup>[1]</sup> These ligands are mostly coordinatively saturated, leaving little room for divergence from the synthetic path encoded into the ligand. This contrasts with most of the systems appearing in the recent literature, which result from unpredictable assembly processes with highly coordinatively unsaturated ligands, in which e.g. “O” donors seek out multiple metal contacts through bridging interactions. L2 is based on a design which effectively assembles six-coordinate metal ions in  $[4 \times 4]$  2D square arrays, but the repositioning of the putative bridging oxygen atoms, combined with the incorporation of the bipy end pieces, produces a pocket array which does not favour grid formation in either the Cu<sup>II</sup> or Mn<sup>II</sup> cases. The grid-based information is partly suppressed, but some elements of the grid instructions remain, as indicated by the presence of two  $[2 \times 2]$  square subunits in the structure. The incorporation of bipy ends provides additional sources of  $\pi$  contacts,

which contribute significantly to the assembly. The examination of such alternative structures provides very useful information for the refinement of ligand design, with the goal of producing complex structures to order via a “Lego®”-type self-assembly approach. We are approaching this objective through the extensive modification of pyridazine-based hydrazone ligands, and other ligand systems in this class.

## Experimental Section

**2:** Manganese(II) nitrate hexahydrate (0.07 g, 0.24 mmol) and L2<sup>[13]</sup> (0.05 g, 0.09 mmol) were refluxed in 15 mL of methanol for 5 min followed by the addition of 0.06 g of sodium acetate trihydrate to produce a red solution. The solution was further refluxed for 3.5 h and 0.030 g (0.034 mmol) of sodium dicyanamide was added with no visible changes. On cooling an orange precipitate formed which readily redissolved on addition of 2 mL of water. The mixture was filtered and the filtrate allowed to slowly evaporate for two weeks, affording a microcrystalline orange-red solid. The solid was redissolved in 10 mL of MeOH, filtered, and the filtrate further allowed to evaporate for two weeks producing well defined orange crystals (32 mg, 47%).  $[(C_{28}H_{22}N_{12}O_2)_8Mn_{12}\{N(CN)_2\}_2](NO_3)_8(H_2O)_{24}$  (6172.05); calcd. C 44.37, H 3.39, N 24.96; found (dried sample) C 44.03, H 3.34, N 25.14.

**Crystal Structure Data for 2:**  $C_{228}H_{222}Mn_{12}N_{110}O_{70}$ , crystal size:  $0.30 \times 0.11 \times 0.11 \text{ mm}$ , triclinic,  $P\bar{1}$  (#2),  $a = 19.080(6)$ ,  $b = 19.085(6)$ ,  $c = 20.978(6) \text{ Å}$ ,  $\alpha = 105.588(7)^\circ$ ,  $\beta = 91.483(7)^\circ$ ,  $\gamma = 102.470(3)^\circ$ ,  $V = 7156(4) \text{ Å}^3$ ,  $T = 123(1) \text{ K}$ ,  $Z = 1$ ,  $\rho_{\text{calcd.}} = 1.458 \text{ g cm}^{-3}$ ,  $\mu(\text{Mo-K}\alpha) = 6.07 \text{ cm}^{-1}$ , 54840 reflections collected, 24868 were unique ( $R_{\text{int}} = 0.0478$ ),  $R1 = 0.0832$ ,  $wR2 = 0.2692$  and 18956 with  $I > 2\sigma(I)$ .

CCDC-784256 (squeezed) and -784257 (unsqueezed) contain the supplementary crystallographic data for this paper. These data can be obtained free of charge from The Cambridge Crystallographic Data Centre via [www.ccdc.cam.ac.uk/data\\_request/cif](http://www.ccdc.cam.ac.uk/data_request/cif).

**Supporting Information** (see also the footnote on the first page of this article): Full experimental details including MS, IR and CHN data. Figure S1 (structure of **1**), Figures S2, S3, S5 ( $\pi$  contacts), Figure S4 (H-bonding contacts); Tables S1, S2 ( $\pi$ -centroid contacts).

## Acknowledgments

The Canadian Natural Sciences and Engineering Research Council (NSERC) is acknowledged for financial support (Grant # 1031-07).

- [1] L. N. Dawe, K. V. Shuvaev, L. K. Thompson, *Chem. Soc. Rev.* **2009**, 38, 2334–2359.
- [2] M. Ruben, J. Rojo, F. J. Romero-Salguero, L. H. Uppadine, J.-M. Lehn, *Angew. Chem. Int. Ed.* **2004**, 43, 3644–3662.
- [3] M. Ruben, J.-M. Lehn, P. Müller, *Chem. Soc. Rev.* **2006**, 35, 1056–1067.
- [4] C. J. Matthews, K. Avery, Z. Xu, L. K. Thompson, L. Zhao, D. O. Miller, K. Biradha, K. Poirier, K. J. Zaworotko, C. Wilson, A. E. Goeta, J. A. K. Howard, *Inorg. Chem.* **1998**, 37, 5266–5276.
- [5] L. K. Thompson, C. J. Matthews, L. Zhao, Z. Xu, D. O. Miller, C. Wilson, M. Leech, J. A. K. Howard, S. L. Heath, A. G.

- Whittaker, R. E. P. Winpenny, *J. Solid State Chem.* **2001**, *159*, 308–320.
- [6] V. A. Milway, S. M. T. Abedin, V. Niel, T. L. Kelly, L. N. Dawe, S. K. Dey, D. W. Thompson, D. O. Miller, M. S. Alam, P. Müller, L. K. Thompson, *Dalton Trans.* **2006**, 2835–2851.
- [7] S. K. Dey, L. K. Thompson, L. N. Dawe, *Chem. Commun.* **2006**, 4967–4969.
- [8] L. N. Dawe, L. K. Thompson, *Angew. Chem. Int. Ed.* **2007**, *46*, 7440–7444.
- [9] S. K. Dey, T. S. M. Abedin, L. N. Dawe, S. S. Tandon, J. L. Collins, L. K. Thompson, A. V. Postnikov, M. S. Alam, P. Müller, *Inorg. Chem.* **2007**, *46*, 7767–7781.
- [10] L. N. Dawe, K. V. Shuvaev, L. K. Thompson, *Inorg. Chem.* **2009**, *48*, 3323–3341.
- [11] a) F. J. M. Hoebe, P. Jonkheijm, E. W. Meijer, A. P. H. Schenning, *Chem. Rev.* **2005**, *105*, 1491–1546; b) L. Brammer, *Chem. Soc. Rev.* **2004**, *33*, 476–489; c) V. A. Milway, T. S. M. Abedin, L. K. Thompson, D. O. Miller, *Inorg. Chim. Acta* **2006**, *359*, 2700–2711; d) C. G. Claessens, J. F. Stoddart, *J. Phys. Org. Chem.* **1997**, *10*, 254–272; e) E. A. Meyer, R. K. Castellano, F. Diedrich, *Angew. Chem. Int. Ed.* **2003**, *42*, 1210–1250; f) M. J. Hannon, *Chem. Soc. Rev.* **2007**, *36*, 280–295; g) S. Mizyed, P. E. Georghiou, M. Bancu, B. Cuadra, A. K. Rai, P. Cheng, L. T. Scott, *J. Am. Chem. Soc.* **2001**, *123*, 12770–12774; h) P. E. Georghiou, A. H. Tran, S. Mizyed, M. Bancu, L. T. Scott, *J. Org. Chem.* **2005**, *70*, 6158–6163; i) A. Sygula, F. R. Fronczek, R. Sygula, P. W. Rabideau, M. M. Olmstead, *J. Am. Chem. Soc.* **2007**, *129*, 3842–3843.
- [12] N. Inukai, J. Yuasa, T. Kawai, *Chem. Commun.* **2010**, *46*, 3929–3931.
- [13] K. V. Shuvaev, S. S. Tandon, L. N. Dawe, L. K. Thompson, *Chem. Commun.* **2010**, *46*, 4755–4757.
- [14] Z. Xu, K. He, L. K. Thompson, O. Waldmann, *MAG-MUN4.11*, generalized software package for spin-exchanged clusters, Memorial University, St. John's, Newfoundland, **2005**.

Received: August 3, 2010

Published Online: September 10, 2010